

# Impurity induced Modulational instability in Bose-Einstein condensates

Ishfaq Ahmad Bhat, Bishwajyoti Dey

*Department of Physics, Savitribai Phule Pune University, Pune 411007, Maharashtra, India*

---

## Abstract

By means of linear stability analysis (LSA) and direct numerical simulations of the coupled Gross-Pitaevskii (GP) equations, we address the impurity induced modulational instability (MI) and the associated nonlinear dynamics in Bose-Einstein condensates (BECs). We explore the dual role played by the impurities within the BECs —the instigation of MI and the dissipation of the initially generated solitary waves. Because of the impurities, the repulsive BECs are even modulationally unstable and this tendency towards MI increases with increasing impurity fraction and superfluid-impurity coupling strength. However, the tendency of a given BEC towards the MI decreases with the decreasing mass of the impurity atoms while the sign of the superfluid-impurity interaction plays no role. The above results are true even for attractive BECs except for a weak superfluid-impurity coupling, where the MI phenomenon is marginally suppressed by the presence of impurities. The dissipation of the solitons reduces their lifetime and is eminent for a larger impurity fraction and strong superfluid-impurity strength respectively.

*Keywords:* Modulational Instability, solitons, Bose-Einstein Condensates, coupled Gross-Pitaevskii Equation

---

## 1. Introduction

Modulational instability (MI) is the most prevalent phenomenon in nonlinear systems [1] wherein a continuous wave background becomes unstable against the growth of weak perturbations. As a result, localized solitary waves are formed due to the interplay between the intrinsic nonlinearity and dispersion. Although MI has been studied in nonlinear fibre optics [2], fluid dynamics [3], plasma [4], and even scattering phenomena [5], the MI in BECs has recently received great attention both theoretically [6, 7, 8, 9, 10] and experimentally [11, 12]. A variety of BEC applications, such as quantum phase transitions [13], matter-wave amplification [14], atom interferometry [15] and atom lasers [16] result from the efficient manipulation of the matter wave dynamics of an ultracold BEC by external fields. The MI in BECs and its associated dynamics is well described by the mean-field Gross-Pitaevskii (GP) equation which is nonlinear in nature. Scalar BECs are governed by the single component GP equations while the multicomponent BECs are described by coupled GP equations. The nonlinearity in a BEC is introduced via the  $s$ -wave interactions that are manipulated precisely in experiments by the optical [17, 18] and magnetic [19, 20] Feshbach resonances. In addition to accounting for the MI in BECs, the GP equation exhibits different types of nonlinear structures, including solitons [21, 22] and vortices [23, 24].

The presence of impurities in BECs offer a platform to investigate mass-imbalanced multicomponent systems [25, 26, 27, 28]. The impurity-superfluid interactions in these imbalanced BEC systems realize Bose polarons which under strong interactions result into impurity-solitons [29]. The impurity-superfluid systems are also central towards the understanding of Kondo effect [30], spin transport [31], spin-charge separation [32] and synthetic superfluid chemistry [33]. While the number of impurities in a BEC can be fixed either by the controlled doping [34] or by transferring coherently a fraction of the condensate atoms from one hyperfine level to another by means of a radio-frequency (rf) pulse [35].

The earlier works addressing MI in single component BECs [7, 36, 37] dictate that MI is a natural precursor to the formation of bright solitons. In a single component BEC, MI is possible only for a focusing (attractive) nonlinearity [38, 39]. By tuning the atomic interactions in a BEC from repulsive to attractive, MI results in the formation of bright matter-wave solitons [21, 11, 40]. In a binary BEC, MI is possible even for repulsive interactions whereby dark-bright solitary wave complexes are formed if the self-repulsion of each component is outbalanced by the cross-repulsion

between the two components [41, 8, 10]. The dark-bright soliton complexes are coherent structures consisting of a bright soliton in one component effectively trapped by a dark soliton in the second component. This results in the formation of domain walls which realize the phase separation in the immiscible binary BEC [8, 10, 42, 43]. The MI phenomenon has also been studied extensively in BECs with synthetic gauge potentials [44, 45]. In presence of gauge potentials, MI occurs even in the miscible binary BECs. Recently, the MI analysis has been extended to dipolar [46, 47] and density-dependent BECs [48]. In dipolar BECs, the MI results in the formation of quantum droplets while in density-dependent BECs unidirectionally moving chiral solitons are obtained.

In the framework of the mean-field approach, this paper addresses the MI and the associated nonlinear dynamics of solitary wave formation in an effectively one-dimensional superfluid-impurity system. We consider a binary BEC system in which the condensate (superfluid) interacts with a dilute fraction (0-6%) of impurity atoms. When the impurity fraction in a BEC exceeds 0.2%, the impurity atoms are also Bose-condensed [35]. The MI analysis in a binary BEC has usually been carried out for an equal distribution of atoms in the two components [8, 13, 44]. However, by varying the impurity fraction and their interaction with the superfluid, we study the effect of mass imbalance on the MI phenomena in the BECs. Moreover, the impurity atoms can be either heavier or lighter or of the same mass as the superfluid atoms. A unit mass ratio can be achieved by transferring coherently a small fraction of superfluid atoms into another hyperfine state. Such a situation is neatly modelled by the experiments of Aycock [35] and Jørgensen [26]. By considering different superfluid-to-impurity atomic mass ratios, we additionally study its effect on the impurity-induced MI in BECs.

The subsequent material is structured as follows. Section 2 introduces the model and the corresponding coupled GP equations. The dispersion relation produced by the linear stability analysis (LSA) is derived and discussed. Section 3 reports the results of numerical simulations of the system under consideration. The paper is concluded by Sec. 4.

## 2. Model and MI Analysis

We consider a one-dimensional (1D) BEC with atomic mass  $m_1$  and consisting of  $N_1$  atoms in a state  $\psi_1$  collisionally coupled to  $N_2$  Bose-condensed impurity atoms of mass  $m_2$  in the state  $\psi_2$ . Such a projected BEC system is described by the following coupled GP equations [33, 35]:

$$i\hbar \frac{\partial \psi_1}{\partial t} = \left( -\frac{\hbar^2}{2m_1} \frac{\partial^2}{\partial x^2} + u_1 |\psi_1|^2 + u_{12} |\psi_2|^2 \right) \psi_1 \quad (1a)$$

$$i\hbar \frac{\partial \psi_2}{\partial t} = \left( -\frac{\hbar^2}{2m_2} \frac{\partial^2}{\partial x^2} + u_{12} |\psi_1|^2 \right) \psi_2 \quad (1b)$$

The nonlinear coefficient  $u_1 = 2\hbar^2 a_1 / (m_1 a_\perp^2)$  specifies the interaction between the superfluid atoms in state  $\psi_1$  and  $u_{12} = 2\hbar^2 a_{12} / m_{12} (a_\perp^2 + b_\perp^2)$  with  $m_{12}^{-1} = m_1^{-1} + m_2^{-1}$ , determines the coupling between the superfluid and impurity atoms. Here  $a_1$  and  $a_{12}$  are the characteristic scattering lengths while  $a_\perp = \sqrt{\hbar/m_1 \omega_\perp}$  and  $b_\perp = \sqrt{\hbar/m_2 \omega_\perp}$  are the harmonic oscillator lengths such that  $\omega_\perp$  is the transverse trapping frequency. The number of atoms in each state is conserved by the normalization,  $\int dx |\psi_i(x)|^2 = N_i$  and  $N = N_1 + N_2$  is the total number of atoms. Further, the impurity fraction  $N_2/N_1$  is kept very low (within a few percent) in experiments and is varied by tuning the rf-amplitude [35]. Accordingly, we neglect the interactions between the impurity atoms. By means of spatiotemporal scaling [49],  $t = \omega_\perp^{-1} t'$ ,  $x = a_\perp x'$ , and  $\psi_i = \psi'_i / \sqrt{|a_\perp|}$ , Eqs. (1a) and (1b) can be recast in the following form:

$$i \frac{\partial \psi_1}{\partial t} = \left( -\frac{1}{2} \frac{\partial^2}{\partial x'^2} + g_1 |\psi_1|^2 + g_{12} |\psi_2|^2 \right) \psi_1 \quad (2a)$$

$$i \frac{\partial \psi_2}{\partial t} = \left( -\frac{\rho}{2} \frac{\partial^2}{\partial x'^2} + g_{12} |\psi_1|^2 \right) \psi_2 \quad (2b)$$

where  $\rho = m_1/m_2$  denotes the mass ratio. In this study, we consider the mass ratios,  $\rho = \{1/2, 1, 2\}$ . These correspond to the experimentally relevant cases of  $^{14}\text{K}-^{87}\text{Rb}$ ,  $^{87}\text{Rb}-^{87}\text{Rb}$  and  $^{87}\text{Rb}-^{14}\text{K}$  superfluid-impurity systems respectively. The higher mass ratios of  $\rho = 3$  and  $4$  apply respectively to the  $^{133}\text{Cs}-^{41}\text{K}$  and  $^{87}\text{Rb}-^{23}\text{Li}$  mixtures. In the resulting dimensionless GP equations the primes have been omitted and have the same structure as above, but with  $\hbar = m = 1$ . The scaled coupling coefficients are now defined by,  $g_1 = 2a_1/a_\perp$  and  $g_{12} = 4a_{12}/a_\perp$ .

In the context of LSA of Eqs. (2a) and (2b), we examine the MI in a BEC system with  $n_{10}$  and  $n_{20}$  as uniform densities of the superfluid and impurity atoms *i.e.*,  $\psi_j = \sqrt{n_{j0}}e^{-i\mu_j t}$  for  $j = 1, 2$ . In terms of the equilibrium densities, chemical potentials,  $\mu_1 = g_1 n_{10} + g_{12} n_{20}$  and  $\mu_2 = g_{12} n_{20}$ . For the perturbed wave functions of the form,  $\psi_j = (\sqrt{n_{j0}} + \delta\psi_j)e^{-i\mu_j t}$ , the linearized equations for the perturbations are:

$$i\frac{\partial\delta\psi_1}{\partial t} = -\frac{1}{2}\frac{\partial^2\delta\psi_1}{\partial x^2} + g_1 n_{10}(\delta\psi_1 + \delta\psi_1^*) + g_{12}\sqrt{n_{10}n_{20}}(\delta\psi_2 + \delta\psi_2^*) \quad (3a)$$

$$i\frac{\partial\delta\psi_2}{\partial t} = -\frac{\rho}{2}\frac{\partial^2\delta\psi_2}{\partial x^2} + g_{12}\sqrt{n_{10}n_{20}}(\delta\psi_1 + \delta\psi_1^*) \quad (3b)$$

where “\*” denotes the complex conjugate. We consider the perturbations in the form of plane waves,  $\delta\psi_j = a_j\text{Cos}(kx - \Omega t) + b_j\text{Sin}(kx - \Omega t)$  with real wavenumber  $k$ , complex eigenfrequency  $\Omega$  and  $j = 1, 2$ . Substituting this in Eqs. (3a) and (3b) results in the following dispersion relation for eigenfrequency,  $\Omega$ :

$$\Omega^4 - \Omega^2 k^2 \left( \frac{k^2}{4}(\rho^2 + 1) + g_1 n_{10} \right) + \frac{k^4 \rho}{4} \left( \frac{k^4 \rho}{4} + g_1 n_{10} \rho - 4n_{10} n_{20} g_{12}^2 \right) = 0 \quad (4)$$

Quartic Eq. (4) for the eigenfrequency,  $\Omega$  can be solved for its roots and results in:

$$\Omega_{\pm}^2 = \frac{k^2}{2} \left( \frac{k^2(\rho^2 + 1)}{4} + g_1 n_{10} \left( 1 \pm \sqrt{1 + 4\delta g^2 \delta n - \frac{k^2 \Delta}{2g_1 n_{10}} + \frac{k^4 \Delta^2}{16g_1^2 n_{10}^2}} \right) \right) \quad (5)$$

where  $\delta g = g_{12}/g_1$  is the interaction ratio,  $\delta n = n_{20}/n_{10}$  represents the mass imbalance and  $\Delta = \rho^2 - 1$ . Eq. (5) which governs the propagation of perturbations on the top of continuous wave solutions may be positive or negative depending on the nature of interactions and mass imbalance. The continuous wave solutions are stable if  $\Omega_{\pm}^2 > 0$  for all real  $k$ . On the other hand, the instability gain is defined as  $\xi = |\text{Im}(\Omega_{\pm})|$ . In case of scalar BECs without an impurity ( $\delta g = \delta n = \Delta = 0$ ), Eq. (5) reproduces the well-known results of MI in dilute BECs where it occurs for an attractive interaction ( $g_1 < 0$ ) in the wavenumber range  $0 < k < 2\sqrt{|g_1 n_{10}|}$  [2, 7, 36]. The maximum MI gain,  $\xi_{\text{max}} = n_{10}|g_1|$  is attained for  $k_{\text{max}} = \sqrt{2n_{10}|g_1|}$ .

The effect of the impurities on the MI in BECs can be analyzed in the framework of Eq. (5) whereby it is evident that the BEC is modulationally unstable even for  $g_1 > 0$ . This situation is of peculiar importance since the scalar ( $\delta g = 0$ ) [7] and miscible binary BECs ( $\delta g < 1$ ) [10] with repulsive  $g_1$  interactions are modulationally stable. A plot of Eq. (5) shown in Figs. 1 (a)-(c) display the variation of the MI gain with the nature and concentration of the impurities in a repulsive BEC with weak superfluid-impurity coupling ( $\delta g < 1$ ). Here the instability is accounted for by  $\Omega_-$  perturbations only and occurs in the wavenumber range  $0 < k < \sqrt{2g_1 n_{10}(-1 + \sqrt{1 + 4\delta g^2 \delta n/\rho})}$ . It is evident from Fig. 1(a)-(c) that for a fixed interaction,  $\delta g$  and atomic mass,  $\rho$  ratios, the MI gain and bandwidth increases with the fraction of impurities in the BEC. In the simplest case of  $\rho = 1$ , the largest MI gain,

$$\xi_{\text{max}} = \text{Im} \left( \sqrt{g_1^2 n_{10}^2 (-1 - 2\delta g^2 \delta n + \sqrt{1 + 4\delta g^2 \delta n})/2} \right) \quad (6)$$

is attained at,

$$k_{\text{max}} = \sqrt{-g_1 n_{10} + g_1 n_{10} \sqrt{1 + 4\delta g^2 \delta n}}. \quad (7)$$

Moreover, the MI gain and the instability bandwidth decreases with the mass ratio,  $\rho$  as shown in Fig 2. Consequently, the values of  $k_{\text{max}}$  also decrease with  $\rho$ . It is worth mentioning that the MI in such BEC systems are also independent of the sign of  $g_{12}$ , though the tendency of the system against the growth of the perturbations increase together with the ratio  $\delta g$ . By comparing Figs. 1(a,b,c) and 1(d,e,f) respectively, it is evident that the MI gain for a given fraction of impurities are considerably larger for a stronger superfluid-impurity coupling ( $\delta g > 1$ ).

In an attractive BEC with  $g_1 < 0$ , the modulational instability is accounted for by  $\Omega_+$  perturbations and occurs in the wavenumber range  $0 < k < \sqrt{2g_1 n_{10}(-1 - \sqrt{1 + 4\delta g^2 \delta n/\rho})}$  as shown in Fig. 3. It is evident from Fig. 3(a)-(c)

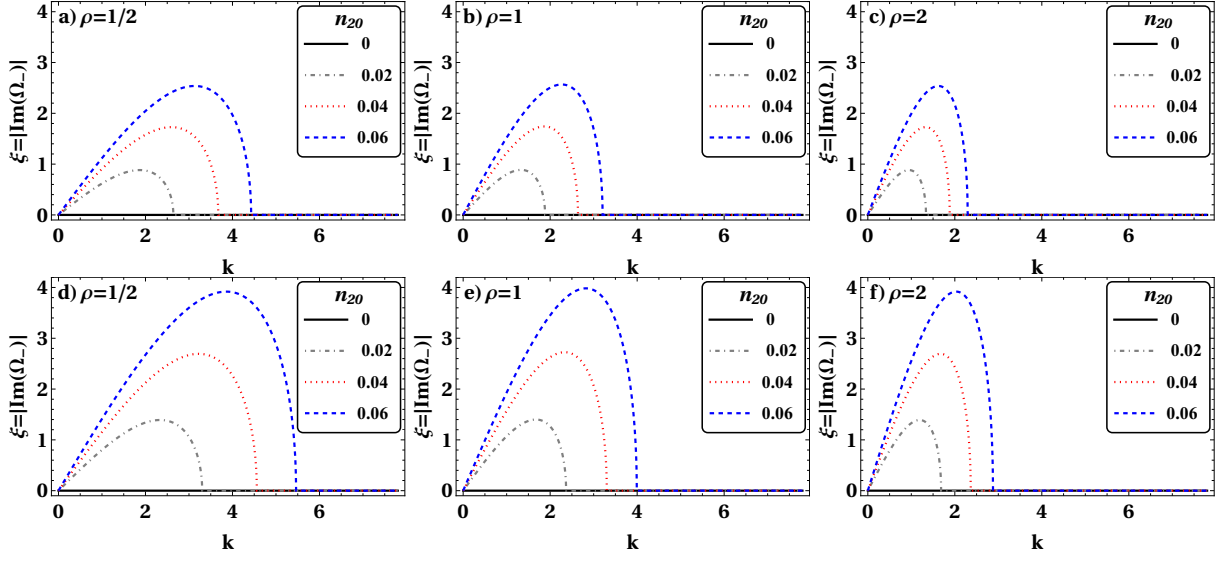


Figure 1: The MI gain corresponding to the  $\Omega_-$  perturbation branch for  $g_1 = 50$  and different impurity concentrations,  $n_{20}$ . The superfluid-impurity coupling is fixed at  $\delta g = 0.95$  in (a)-(c) and  $\delta g = 1.2$  in (d)-(f) respectively, while  $n_{10} + n_{20} = 1$ . Note that the repulsive scalar BECs with  $n_{20} = 0$  are always modulationally stable.

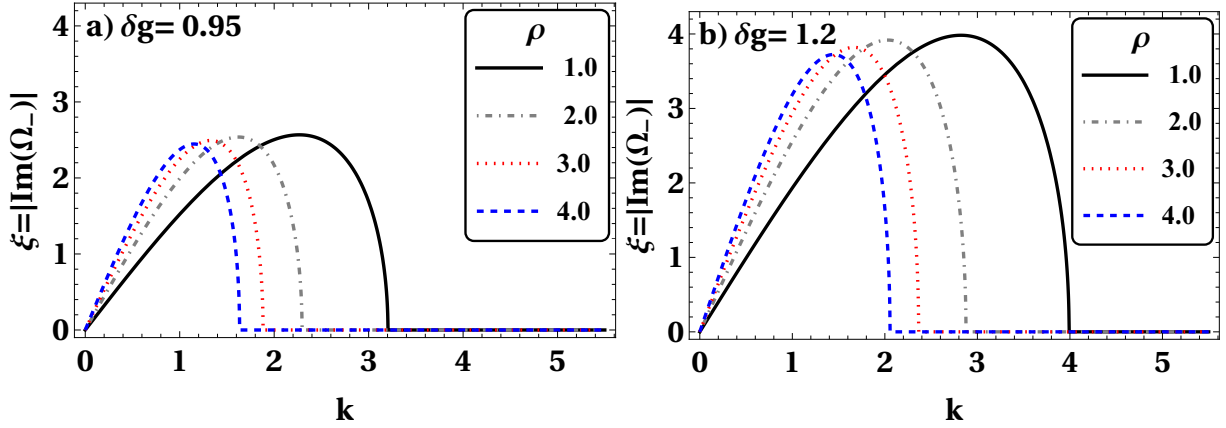


Figure 2: Variation of the MI gain with atomic mass ratio,  $\rho$  in a BEC with a) weak ( $\delta g < 1$ ) and b) strong ( $\delta g > 1$ ) superfluid-impurity interactions. The impurity fraction,  $n_{20} = 0.06$  in each case.

that the MI gain is marginally suppressed with the impurity concentration if  $\delta g < 1$  while for  $\delta g > 1$ , the largest MI gain and the instability bandwidth increases with increasing impurity fraction in the attractive BECs as shown in Fig. 3(d)-(f). These modifications to the already existing MI in an attractive BEC due to the impurity fraction can be further understood by considering  $\rho = 1$ . In such a case, the largest MI gain,

$$\xi_{\max} = \text{Im} \left( \sqrt{-g_1^2 n_{10}^2 (1 + 2\delta g^2 \delta n + \sqrt{1 + 4\delta g^2 \delta n}) / 2} \right) \quad (8)$$

is attained at,

$$k_{\max} = \sqrt{-g_1 n_{10} - g_1 n_{10} \sqrt{1 + 4\delta g^2 \delta n}}. \quad (9)$$

A plot of Eq. (9) in Fig. 4(a) shows the variation of  $k_{\max}$  with the impurity fraction,  $n_{20}$  for both  $\delta g < 1$  and  $\delta g > 1$ . Notice that  $k_{\max}$  and hence  $\xi_{\max}$  (not shown in Fig. 4) decreases linearly together with  $n_{20}$  in case  $\delta g < 1$  while it

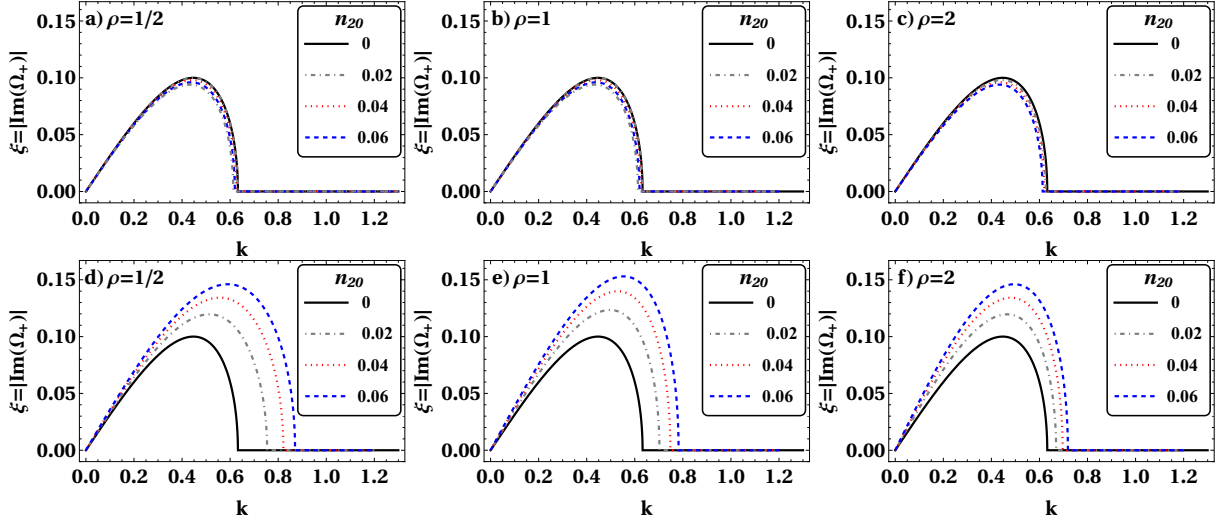


Figure 3: The MI gain corresponding to the  $\Omega_+$  perturbation branch for  $g_1 = -0.1$  and different impurity concentrations,  $n_{20}$ . The superfluid-impurity coupling is fixed at  $\delta g = 0.05$  in (a)-(c) and  $\delta g = 4.0$  in (d)-(f) respectively, while  $n_{10} + n_{20} = 1$ . Note that scalar BECs with attractive interactions and  $n_{20} = 0$  are always modulationally unstable.

increases non-linearly when  $\delta g > 1$ . The same is true for higher values of  $\rho$  as shown in Fig. 4(b), except that the  $k_{\max}$  values are lower for the corresponding values of impurity fraction. Like in case of BECs with repulsive interactions, the MI gain and instability bandwidth decrease with  $\rho$  for a fixed impurity fraction.

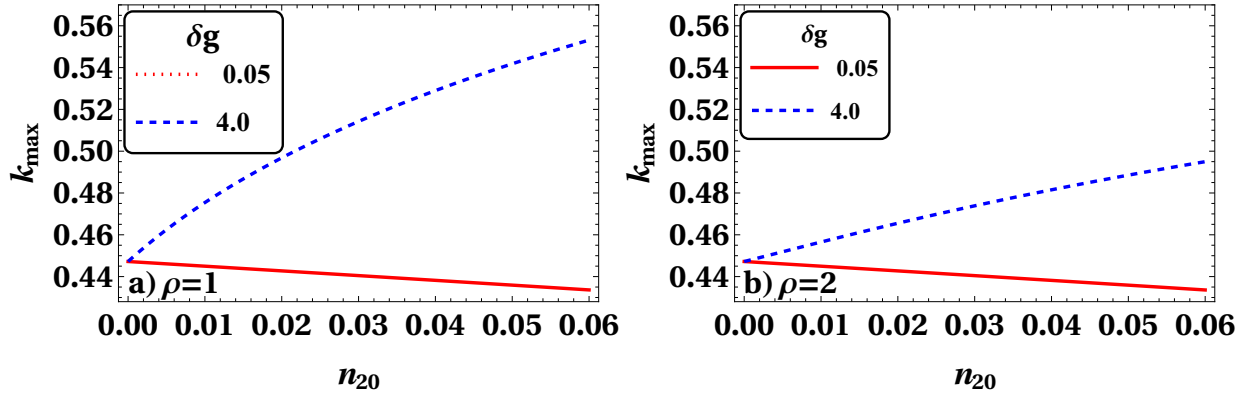


Figure 4: Variation of  $k_{\max}$  with the concentration of impurities,  $n_{20}$  for  $g_1 = -0.1$ , (a)  $\rho = 1$  and (b)  $\rho = 2$ .

### 3. Numerics

In this section, we discuss the nonlinear dynamics caused by impurity-induced MI in the BECs. We solve Eqs. (2a) and (2b) numerically by employing FFTW [50] mediated split-step fast-Fourier method [51]. Throughout the simulations, we set the time step  $\Delta t = 0.001$  and the spatial grid size  $\Delta x = L/N_s$  with  $N_s = 2048$ . The domain size,  $L = 200$  and  $100$  is respectively chosen for repulsive ( $g_1 > 0$ ) and attractive ( $g_1 < 0$ ) BECs. Initial continuous wave background with impurity fraction ranging from 0-6% is studied for its MI by seeding weak and random perturbations for different strengths of  $g_1$  and  $\delta g$  in the following subsections.

### 3.1. $g_1 > 0$ and $\delta g < 1$

The MI analysis discussed in the previous section shows that impurities within a BEC make it vulnerable towards the growth of perturbations (MI) even for repulsive  $g_1$  interactions and  $\delta g < 1$ . In this regard, Fig. 5(a)-(c) shows the time development of the initially perturbed  $\rho = 1$  continuous wave density for 2%, 4% and 6% impurity concentrations respectively. For a given value of  $g_1 = 50$  and  $\delta g = 0.95$ , it is evident that the BEC realizes phase separation through the formation of dark solitary waves. This is because of the repulsive superfluid-impurity coupling and the density modulation grows out of phase between the two components. This density disturbance in the superfluid increases with the increasing concentration of the impurities. Consequently, the number of phase-separated domains or solitary waves increases proportionately with the concentration of the impurities such that for a 2% impurity, a pair of parallel dark-solitons appear at  $t_{\text{MI}} > 900$ . The critical time at which MI-induced solitary waves start appearing decreases with the increasing concentration of impurities. Though the impurities felicitate the MI phenomena in BECs, these are also responsible for the dissipation and Brownian motion of the generated solitary waves [35]. Fig. 5(c) shows that one of the several generated solitary waves in the superfluid executes zig-zag motion during its evolution and finally disappears due to the dissipation by impurities. Since,  $\delta g < 1$ , the dissipation and the Brownian motion of the solitary waves due to the impurities is not prominent, though it increases with the concentration of the impurities. Similar outcomes are observed in the lower panel (Fig. 5(d)-(f)) where  $\rho = 2$ . However, in accordance with the analytical results, the number of initially generated dark solitons is less than those produced in the corresponding simulations with  $\rho = 1$ .

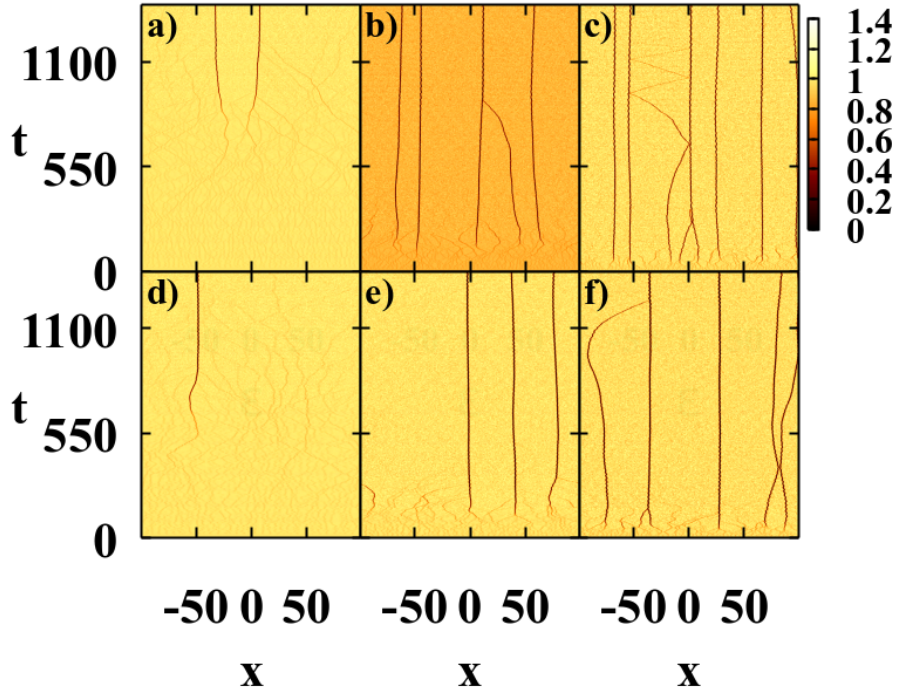


Figure 5: The evolution of the condensate density  $|\psi_1|^2$  due to the development of the MI by a) 2%, b) 4%, and c) 6% impurities respectively in the coordinate space. The upper panel (a)-(c) corresponds to  $\rho = 1$  while the lower panel (d)-(f) represents the corresponding densities with  $\rho = 2$ . The superfluid-impurity coupling is maintained at  $\delta g = 0.05$ . The number of solitons increases together with the impurity fraction and decreases with the mass ratio,  $\rho$ . The dissipation of the generated solitons is negligible for a weaker superfluid-impurity coupling.

### 3.2. $g_1 > 0$ and $\delta g > 1$

The condition  $\delta g > 1$  refers when superfluid-impurity coupling outbalances the interaction between the superfluid atoms. From Eq. (5) it is clear that the MI gain increases with the increase in  $\delta g$  for a fixed value of  $\rho$  and impurity concentration. By comparing the corresponding plots in Fig. 5 and Fig. 6, it is clear that the number of generated

solitary waves is more for a larger superfluid-impurity coupling ( $\delta g$ ). Moreover, when the superfluid-impurity interaction is large, the dissipation due to the impurity atoms within the BEC is also large. Fig. 6 shows that dark solitons within the superfluid component dissipate after executing the zig-zag motion. As the number of impurities in a BEC increases, more solitons in the superfluid dissipate during their time evolution. This consequently reduces the lifetime of the generated solitons. Further, by comparing the corresponding plots in the upper (a-c) and lower (d-f) panels of Fig. 6, it is evident that the number of generated solitons decrease with increasing values of mass ratio,  $\rho$ .

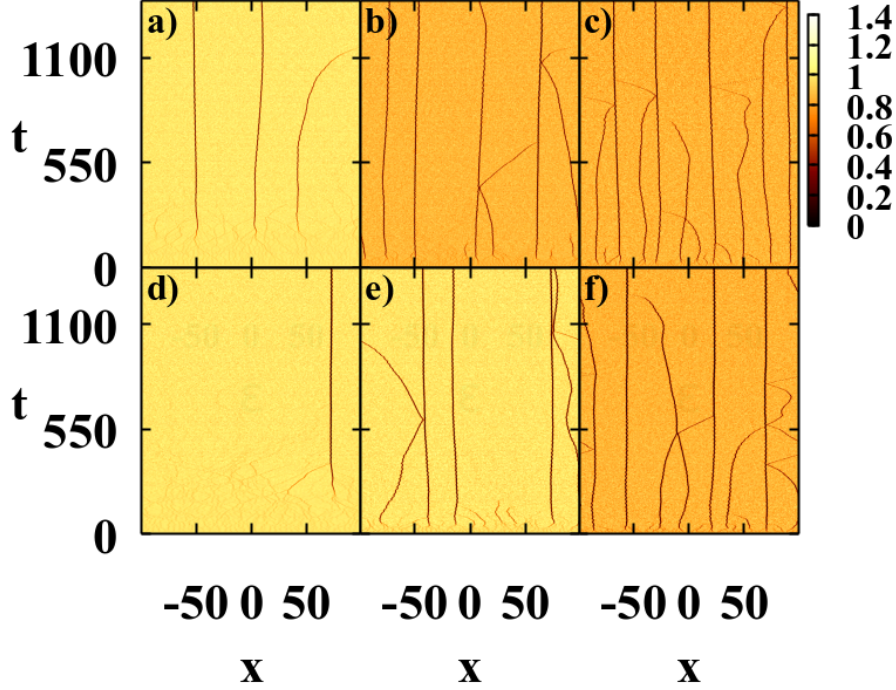


Figure 6: The evolution of the condensate density  $|\psi_1|^2$  due to the development of the MI by a) 2%, b) 4%, and c) 6% impurities respectively in the coordinate space. The upper panel (a)-(c) corresponds to  $\rho = 1$  while the lower panel (d)-(f) represents the corresponding densities with  $\rho = 2$ . The superfluid-impurity coupling is maintained at  $\delta g = 4$ . Both the number of solitons and their dissipation are large for a larger superfluid-impurity coupling.

### 3.3. $g_1 < 0$ and $\delta g < 1$

It is well known that MI in BECs with attractive self-interactions lead to the formation of bright matter-wave solitons. Eq. (5) and Fig. 3 shows that the BEC is modulationally unstable for  $g_1 = -0.1$ . However, the presence of impurities changes the MI in the system only slightly if  $\delta g < 1$ . Fig. 7 shows the spatiotemporal evolution of the initially perturbed continuous wave density for different impurity concentrations and parameters,  $g = -0.1$ ,  $\delta g = 0.05$  and  $\rho = 1$ . It shows the generation of a train of solitons at  $t_{\text{MI}} \geq 205$  in the absence of impurities. In accordance with Eq. (9), the wavenumber corresponding to the initially excited mode is  $k_{\text{max}} \approx 0.45$  as shown in 7(d). This corresponds to  $\lambda_{\text{max}} = 2\pi/k_{\text{max}} \approx 14.19$  and hence,  $n_s = L/\lambda_{\text{max}} \approx 7$  solitons. As the concentration of impurities is increased, it is evident that the critical time,  $t_{\text{MI}}$  at which MI-induced bright solitons start appearing increases slightly due to the slight decrease in the largest MI gain,  $\xi_{\text{max}}$ . With an impurity concentration of 2% and 6% respectively, the largest wavenumber,  $k_{\text{max}} \approx 0.44$  and  $0.43$  correspond to the initially excited modes as shown in Figs. 7(e) and 7(f) respectively. However, due to the slight changes in the MI parameters,  $k_{\text{max}}$  and  $\xi_{\text{max}}$ , the number of initially generated solitons remains the same in all cases. Moreover, due to the weak superfluid-impurity coupling the dissipation is even negligible.

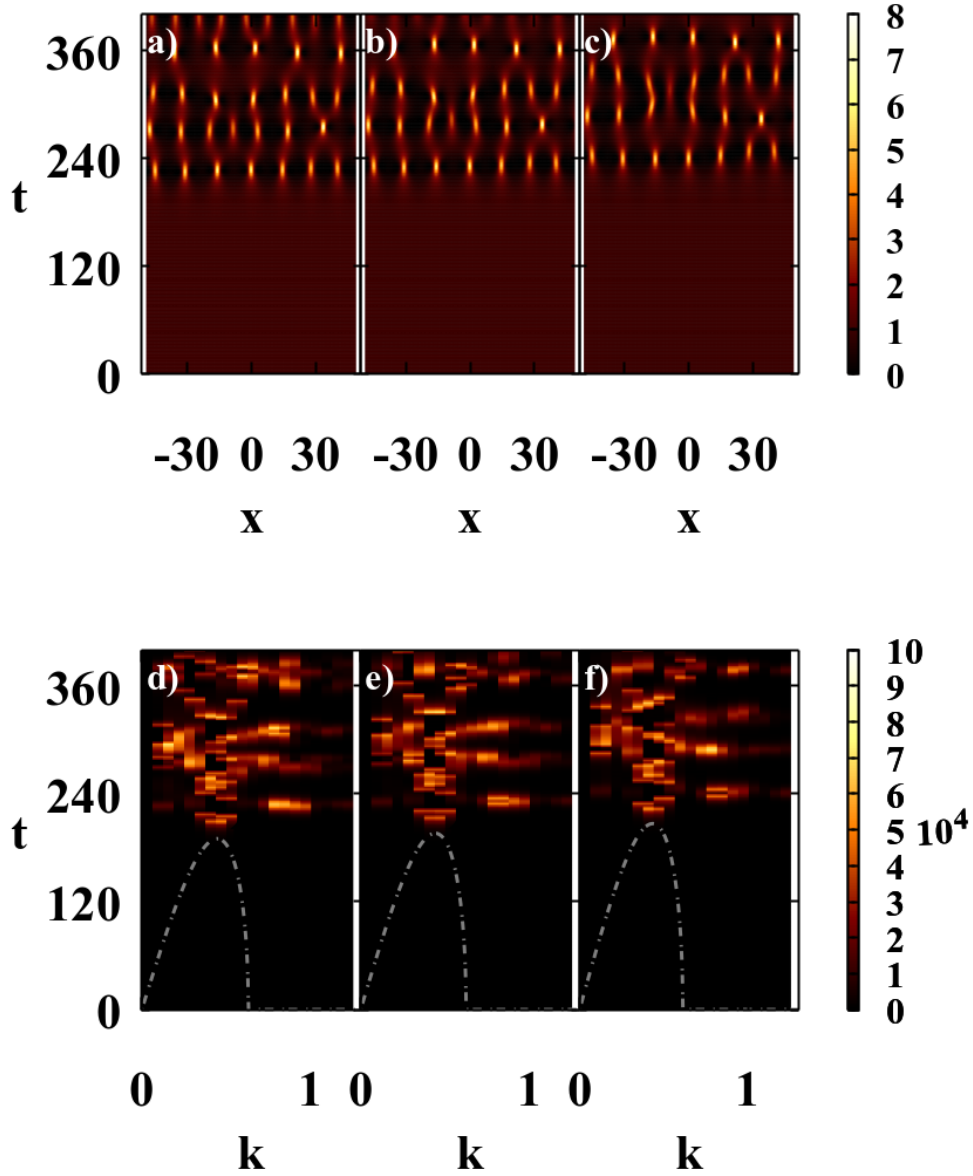


Figure 7: The evolution of the condensate density  $|\psi_1|^2$  due to the development of the MI by a) 0%, b) 2%, and c) 6% impurities respectively in the coordinate space. The lower panel (d)- (f) represents the corresponding densities in  $k$ - space. The superfluid-impurity coupling is maintained at  $\delta g = 0.95$ . For  $\delta g < 1$ , the critical time for the generation of bright solitons increases with the impurity fraction.

#### 3.4. $g_1 < 0$ and $\delta g > 1$

In the previous subsection 3.3, we showed that the impurities do not play a significant role in the MI-associated nonlinear dynamics in attractive BECs for a weak superfluid-impurity coupling ( $\delta g < 1$ ). The same is true for a larger range of  $\delta g > 1$ . In order to explain the effects on the MI due to the impurities, we have here chosen a much stronger superfluid-impurity coupling,  $\delta g = 4$ . Fig. 8 shows the spatiotemporal evolution of the initially perturbed continuous wave density with 0%, 2% and 6% impurity concentrations respectively. The critical time  $t_{\text{MI}}$  decreases with the concentration of impurities. This is due to the increase in the largest MI gain,  $\xi_{\text{max}}$  given by Eq. (8). With an impurity concentration of 0%, 2% and 6% respectively, the largest wavenumber,  $k_{\text{max}} \approx 0.45, 0.49$  and  $0.55$  correspond to the initially excited modes as shown in Fig. 8(d)-(f) respectively. Consequently, the number of initially generated



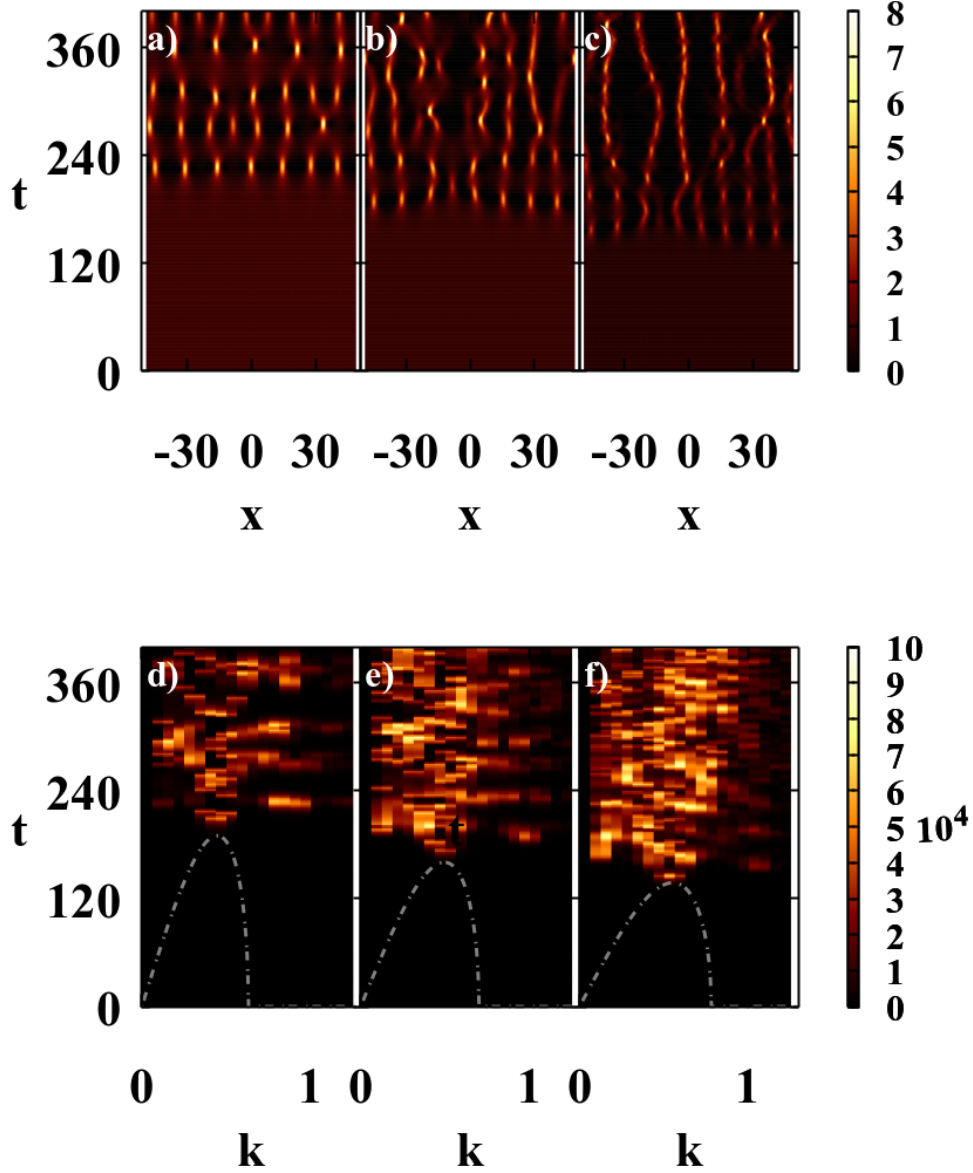


Figure 8: The evolution of the condensate density  $|\psi_1|^2$  due to the development of the MI by a) 0%, b) 2%, and c) 6% impurities respectively in the coordinate space. The lower panel (d)- (f) represents the corresponding densities in  $k$ - space. The superfluid-impurity coupling is maintained at  $\delta g = 1.2$ . For  $\delta g > 1$ , the critical time for the generation of bright solitons decreases with the impurity fraction and there is significant dissipation.

solitons,  $n_s = 7, 8$  and  $9$  respectively. Moreover, due to the strong superfluid-impurity coupling, the dissipation of the generated solitons is prominent. This reduces the lifetime of the solitons and hence the number of solitons decreases with time evolution. The number of initially generated solitons and the critical time for MI development as a function of impurity concentration and the interaction parameters in the numerical simulations for  $\rho = 1$  is summarized in Fig. 9. The MI time always decreases with the impurity concentration and the strength of superfluid-impurity coupling in BECs with repulsive  $g_1$  nonlinearity while in attractive BECs, the MI time either decreases or increases with the impurity fraction, depending on the strength of the superfluid-impurity coupling. In the latter case with  $\delta g < 1$ , the MI time increases while if  $\delta g > 1$  MI time decreases.

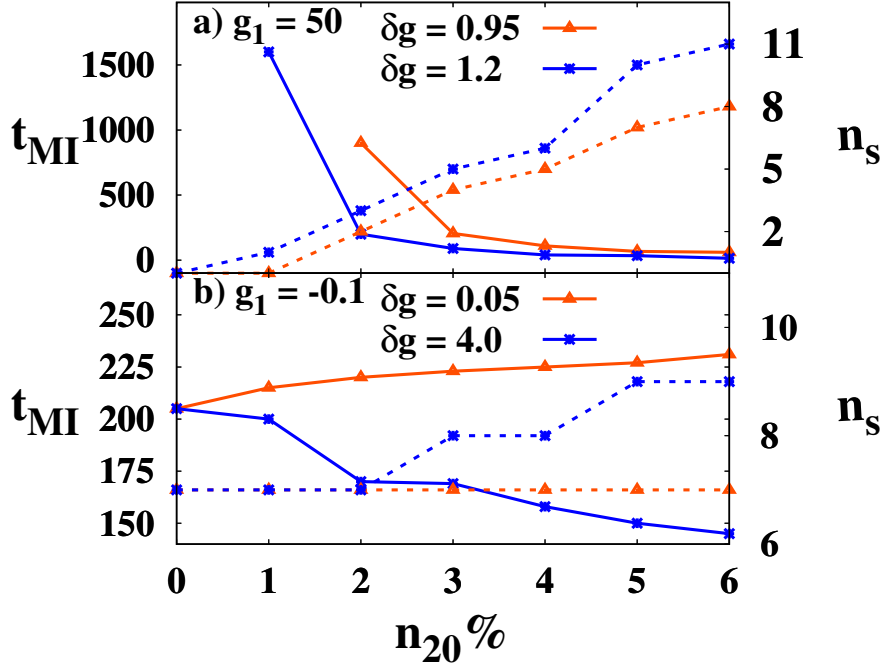


Figure 9: Variation of the MI time,  $t_{\text{MI}}$  (plot-markers with solid lines) and the number of initially generated solitons,  $n_s$  (plot-markers with dashed lines) with impurity concentration,  $n_{20}$  in BECs with  $\rho = 1$ .

#### 4. Conclusion

In summary, we investigated the MI by employing linear stability analysis and direct numerical simulations in a BEC coupled with a dilute fraction of Bose-condensed impurities. Being dilute, the coupling among the impurity atoms is neglected. It is well established that single-component BECs with repulsive interactions are always modulationally stable. Moreover, the binary BECs with an equal proportion of the two components are modulationally unstable iff the cross-phase mediated repulsion between the components outbalances their self-repulsion. However, in the presence of dilute impurities, BECs are always modulationally unstable and is independent of the sign of the superfluid-impurity interaction. The MI induces spatial pattern formation in a repulsive BEC and the generated domains have a solitary wave structure. The tendency of the BEC towards MI increases with the increasing impurity fraction for a fixed superfluid-impurity coupling strength. Consequently, the number of domains increases together with the fraction of impurities in the BEC. Moreover, the MI gain in a given BEC, the instability bandwidth, the number of solitons as well as  $k_{\text{max}}$ , the value of the wave vector  $k$  at which the MI gain attains maximum, decreases with the decreasing mass of the impurity atoms. Despite increasing the tendency of a repulsive BEC towards MI, the impurities are also responsible for the Brownian motion of the solitons and their dissipation. This reduces the lifetime of the solitary wave structures. Naturally, the dissipation is prominent for a greater impurity fraction and increasing superfluid-impurity coupling strength.

As concerns the presence of impurities in attractive BECs slightly affect the preexisting MI phenomena for a weak superfluid-impurity coupling ( $\delta g < 1$ ). The modulational instability time only slightly increases with the impurity fraction. However, for a strong superfluid-impurity coupling ( $\delta g > 1$ ) the modulational instability time decreases and the number of generated solitons increases with the impurity fraction.

#### 5. Acknowledgements

I A Bhat acknowledges CSIR, Government of India, for funding via CSIR Research Associateship (09/137(0627)/2020 EMR-I). BD thanks Science and Engineering Research Board, Government of India for funding through research

project CRG/2020/003787.

## References

- [1] V. E. Zakharov, L. A. Ostrovsky, Modulation instability: the beginning, *Physica D: Nonlinear Phenomena* 238 (5) (2009) 540–548.
- [2] G. Agrawal (Ed.), *Nonlinear Fiber Optics*, 5th Edition, Academic Press, Boston, 2013.
- [3] M. Brunetti, J. Kasparian, Modulational instability in wind-forced waves, *Physics Letters A* 378 (48) (2014) 3626–3630.
- [4] T. Taniuti, H. Washimi, Self-trapping and instability of hydromagnetic waves along the magnetic field in a cold plasma, *Physical review letters* 21 (4) (1968) 209.
- [5] B. A. Malomed, M. Y. Azbel, Modulational instability of a wave scattered by a nonlinear center, *Physical Review B* 47 (16) (1993) 10402.
- [6] V. V. Konotop, M. Salerno, Modulational instability in bose-einstein condensates in optical lattices, *Phys. Rev. A* 65 (2002) 021602.
- [7] G. Theocharis, Z. Rapti, P. Kevrekidis, D. Frantzeskakis, V. Konotop, Modulational instability of gross-pitaevskii-type equations in 1+ 1 dimensions, *Physical Review A* 67 (6) (2003) 063610.
- [8] K. Kasamatsu, M. Tsubota, Multiple domain formation induced by modulation instability in two-component bose-einstein condensates, *Physical review letters* 93 (10) (2004) 100402.
- [9] L. Li, Z. Li, B. A. Malomed, D. Mihalache, W. Liu, Exact soliton solutions and nonlinear modulation instability in spinor bose-einstein condensates, *Physical Review A* 72 (3) (2005) 033611.
- [10] K. Kasamatsu, M. Tsubota, Modulation instability and solitary-wave formation in two-component bose-einstein condensates, *Physical Review A* 74 (1) (2006) 013617.
- [11] P. Everitt, M. Sooriyabandara, M. Guasoni, P. Wigley, C. Wei, G. McDonald, K. Hardman, P. Manju, J. Close, C. Kuhn, et al., Observation of a modulational instability in bose-einstein condensates, *Physical Review A* 96 (4) (2017) 041601.
- [12] I. Ferrier-Barbut, M. Wenzel, M. Schmitt, F. Böttcher, T. Pfau, Onset of a modulational instability in trapped dipolar bose-einstein condensates, *Physical Review A* 97 (1) (2018) 011604.
- [13] R. Kanamoto, H. Saito, M. Ueda, Quantum phase transition in one-dimensional bose-einstein condensates with attractive interactions, *Physical Review A* 67 (1) (2003) 013608.
- [14] S. Inouye, T. Pfau, S. Gupta, A. Chikkatur, A. Görlitz, D. Pritchard, W. Ketterle, Phase-coherent amplification of atomic matter waves, *Nature* 402 (6762) (1999) 641–644.
- [15] B. Anderson, K. Dholakia, E. Wright, Atomic-phase interference devices based on ring-shaped bose-einstein condensates: Two-ring case, *Physical Review A* 67 (3) (2003) 033601.
- [16] E. W. Hagley, L. Deng, M. Kozuma, J. Wen, K. Helmerson, S. Rolston, W. D. Phillips, A well-collimated quasi-continuous atom laser, *Science* 283 (5408) (1999) 1706–1709.
- [17] F. Fatemi, K. Jones, P. D. Lett, Observation of optically induced feshbach resonances in collisions of cold atoms, *Physical Review Letters* 85 (21) (2000) 4462.
- [18] S. Blatt, T. Nicholson, B. Bloom, J. Williams, J. Thomsen, P. Julienne, J. Ye, Measurement of optical feshbach resonances in an ideal gas, *Physical Review Letters* 107 (7) (2011) 073202.
- [19] S. Inouye, M. Andrews, J. Stenger, H.-J. Miesner, D. M. Stamper-Kurn, W. Ketterle, Observation of feshbach resonances in a bose-einstein condensate, *Nature* 392 (6672) (1998) 151–154.
- [20] S. L. Cornish, N. R. Claussen, J. L. Roberts, E. A. Cornell, C. E. Wieman, Stable 85 rb bose-einstein condensates with widely tunable interactions, *Physical Review Letters* 85 (9) (2000) 1795.
- [21] K. E. Strecker, G. B. Partridge, A. G. Truscott, R. G. Hulet, Formation and propagation of matter-wave soliton trains, *Nature* 417 (6885) (2002) 150–153.
- [22] S. Burger, K. Bongs, S. Dettmer, W. Ertmer, K. Sengstock, A. Sanpera, G. V. Shlyapnikov, M. Lewenstein, Dark solitons in bose-einstein condensates, *Physical Review Letters* 83 (25) (1999) 5198.
- [23] M. R. Matthews, B. P. Anderson, P. Haljan, D. Hall, C. Wieman, E. A. Cornell, Vortices in a bose-einstein condensate, *Physical Review Letters* 83 (13) (1999) 2498.
- [24] J. R. Abo-Shaer, C. Raman, J. M. Vogels, W. Ketterle, Observation of vortex lattices in bose-einstein condensates, *Science* 292 (5516) (2001) 476–479.
- [25] J. Catani, G. Lamporesi, D. Naik, M. Gring, M. Inguscio, F. Minardi, A. Kantian, T. Giamarchi, Quantum dynamics of impurities in a one-dimensional bose gas, *Physical Review A* 85 (2) (2012) 023623.
- [26] N. B. Jørgensen, L. Wacker, K. T. Skalmstang, M. M. Parish, J. Levinsen, R. S. Christensen, G. M. Bruun, J. J. Arlt, Observation of attractive and repulsive polarons in a bose-einstein condensate, *Physical review letters* 117 (5) (2016) 055302.
- [27] M.-G. Hu, M. J. Van de Graaff, D. Kedar, J. P. Corson, E. A. Cornell, D. S. Jin, Bose polarons in the strongly interacting regime, *Physical review letters* 117 (5) (2016) 055301.
- [28] J. Akram, A. Pelster, Numerical study of localized impurity in a bose-einstein condensate, *Physical Review A* 93 (3) (2016) 033610.
- [29] S. Shadkhou, R. Bruinsma, Impurities in bose-einstein condensates: From polaron to soliton, *Physical review letters* 115 (13) (2015) 135305.
- [30] A. C. Hewson, *The Kondo Problem to Heavy Fermions*, Cambridge Studies in Magnetism, Cambridge University Press, 1993. doi:10.1017/CB09780511470752.
- [31] M. Zvonarev, V. V. Cheianov, T. Giamarchi, Spin dynamics in a one-dimensional ferromagnetic bose gas, *Physical review letters* 99 (24) (2007) 240404.
- [32] A. Kleine, C. Kollath, I. McCulloch, T. Giamarchi, U. Schollwöck, Spin-charge separation in two-component bose gases, *Physical Review A* 77 (1) (2008) 013607.
- [33] M. Edmonds, M. Eto, M. Nitta, Synthetic superfluid chemistry with vortex-trapped quantum impurities, *Physical Review Research* 3 (2) (2021) 023085.

- [34] N. Spethmann, F. Kindermann, S. John, C. Weber, D. Meschede, A. Widera, Dynamics of single neutral impurity atoms immersed in an ultracold gas, *Physical review letters* 109 (23) (2012) 235301.
- [35] L. M. Ayccock, H. M. Hurst, D. K. Efimkin, D. Genkina, H.-I. Lu, V. M. Galitski, I. Spielman, Brownian motion of solitons in a bose–einstein condensate, *Proceedings of the National Academy of Sciences* 114 (10) (2017) 2503–2508.
- [36] L. Salasnich, A. Parola, L. Reatto, Modulational instability and complex dynamics of confined matter-wave solitons, *Physical review letters* 91 (8) (2003) 080405.
- [37] L. Carr, J. Brand, Spontaneous soliton formation and modulational instability in bose-einstein condensates, *Physical review letters* 92 (4) (2004) 040401.
- [38] J. Higbie, D. Stamper-Kurn, Periodically dressed bose-einstein condensate: A superfluid with an anisotropic and variable critical velocity, *Physical review letters* 88 (9) (2002) 090401.
- [39] U. Al Khawaja, H. Stoof, R. Hulet, K. Strecker, G. Partridge, Bright soliton trains of trapped bose-einstein condensates, *Physical review letters* 89 (20) (2002) 200404.
- [40] J. H. Nguyen, D. Luo, R. G. Hulet, Formation of matter-wave soliton trains by modulational instability, *Science* 356 (6336) (2017) 422–426.
- [41] E. V. Goldstein, P. Meystre, Quasiparticle instabilities in multicomponent atomic condensates, *Physical Review A* 55 (4) (1997) 2935.
- [42] L. Wen, W.-M. Liu, Y. Cai, J. Zhang, J. Hu, Controlling phase separation of a two-component bose-einstein condensate by confinement, *Physical Review A* 85 (4) (2012) 043602.
- [43] I. Vidanović, N. Van Druten, M. Haque, Spin modulation instabilities and phase separation dynamics in trapped two-component bose condensates, *New Journal of Physics* 15 (3) (2013) 035008.
- [44] I. A. Bhat, T. Mithun, B. Malomed, K. Porsezian, Modulational instability in binary spin-orbit-coupled bose-einstein condensates, *Physical Review A* 92 (6) (2015) 063606.
- [45] P. Otlaadisa, C. B. Tabi, T. C. Kofané, Modulation instability in helicoidal spin-orbit coupled open bose-einstein condensates, *Physical Review E* 103 (5) (2021) 052206.
- [46] I. Ferrier-Barbut, H. Kadau, M. Schmitt, M. Wenzel, T. Pfau, Observation of quantum droplets in a strongly dipolar bose gas, *Physical review letters* 116 (21) (2016) 215301.
- [47] M. Schmitt, M. Wenzel, F. Böttcher, I. Ferrier-Barbut, T. Pfau, Self-bound droplets of a dilute magnetic quantum liquid, *Nature* 539 (7628) (2016) 259–262.
- [48] I. A. Bhat, S. Sivaprakasam, B. A. Malomed, Modulational instability and soliton generation in chiral bose-einstein condensates with zero-energy nonlinearity, *Physical Review E* 103 (3) (2021) 032206.
- [49] L. Devassy, C. P. Jisha, A. Alberucci, V. Kuriakose, Parity-time-symmetric solitons in trapped bose-einstein condensates and the influence of varying complex potentials: a variational approach, *Physical Review E* 92 (2) (2015) 022914.
- [50] <http://www.fftw.org/>.
- [51] P. Kaur, A. Roy, S. Gautam, Fortress: Fortran programs for solving coupled gross–pitaevskii equations for spin–orbit coupled spin-1 bose–einstein condensate, *Computer Physics Communications* 259 (2021) 107671.